



# H-polarized plane-wave scattering by a PEC strip grating on top of a dielectric substrate: analytical regularization based on the Riemann-Hilbert Problem solution

Fedir O. Yevtushenko, Sergii V. Dukhopelnykov and Alexander I. Nosich

Laboratory of Micro and Nano Optics, Institute of Radio-Physics and Electronics NASU, Kharkiv, Ukraine

## ABSTRACT

We consider the H-polarized plane wave scattering from an infinite flat grating of perfectly electrically conducting strips, placed on the interface of a dielectric slab. We reduce this problem to a dual series equation for the complex amplitudes of the Floquet spatial harmonics. Then, we perform analytical regularization of this equation, based on the inversion of the static part of the problem with the aid of the Riemann-Hilbert Problem. This yields a Fredholm second-kind infinite matrix equation, numerical solution of which has a guaranteed convergence. Numerical results obtained demonstrate how the rate of convergence depends on the geometrical parameters and then concentrate on the resonance effects in the reflection and transmission. We reveal and discuss ultra-high-Q resonances on the lattice modes of such a composite grating, overlooked in earlier studies.

## ARTICLE HISTORY

Received 23 August 2019  
Accepted 16 January 2020



## KEYWORDS

Strip grating; scattering; regularization

## 1. Introduction

The scattering of plane waves from the infinite flat grating made of perfect electrically conducting (PEC) strips is a canonical problem of computational electromagnetics since a hundred years ago [1]. Within this time, two mathematically grounded approaches that lead to the algorithms possessing the guaranteed convergence have been developed. One of them is based on the method of analytical regularization (MAR) and uses explicit inversion of the static part of the problem, i.e. its most singular part [2]. Such inversion can be performed in several equivalent ways. According to one of them, the problem is reduced to a log-singular or hyper-singular, depending on the polarization, electric-field integral equation (IE). Then, it is discretized using Galerkin projection on the weighted Chebyshev polynomials, which form the set of orthogonal eigen functions of IE static part [3–5]. Important improvements to this technique, related to the computation of the coupling integrals, were introduced in [6,7].

The other way is to reduce the problem to the dual series equation (DSE) for the amplitudes of the Floquet harmonics. Then DSE's static-part inversion is done using the Riemann-Hilbert Problem (RHP) method [8,9]. This way can be also viewed as application

**CONTACT** Fedir O. Yevtushenko  fedir.yevtushenko@gmail.com  Laboratory of Micro and Nano Optics, Institute of Radio-Physics and Electronics NASU, Kharkiv 61085, Ukraine

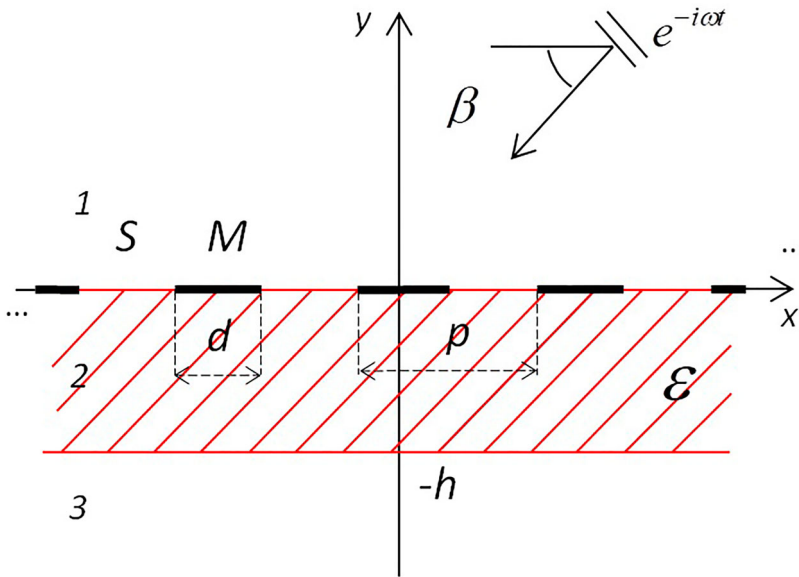


**Figure 1.** The cross-sectional geometry of a flat PEC strip grating on top of a dielectric layer, illuminated by a plane wave.

of the discrete Fourier transform to the previously explained technique. In each case, the resulting infinite-matrix equation is a Fredholm second-kind equation. Then the Fredholm theorems guarantee the convergence in the sense that the larger the matrix truncation order, the closer the solution to exact one, in a certain norm.

The second approach is based on the direct numerical solution of the same singular IEs using the Nystrom-type discretizations and numerical quadratures [10,11]. In this case, the convergence is guaranteed by the theorems of approximation of singular integrals using the quadratures [12,13].

These solutions for the PEC-strip gratings in the free space have been further adapted to treat the imperfect gratings made of resistive (including graphene), impedance, and dielectric strips [9,14–16]. Naturally, this implies using the impedance boundary condition or the generalized boundary condition.

Still in practical situations, strip gratings are usually placed inside a dielectric layer or on top of it – see Figure 1. In the presence of such layer, the corresponding modification of the mentioned above approaches and methods needs some analytical work however is always possible. This is because the IE singularities (related always to the static parts) remain the same. A MAR-RHP approach was first applied to such a problem with PEC strips in [17] although no numerical results were published. Later, it was used in [18,19] to study PEC strip gratings on the top of chiral and magnetic layer, respectively.

The examples of the MAR-Galerkin solutions of that kind can be found in [19–27]. In some of the mentioned above works, extremely sharp resonances can be spotted in the numerical results for the H and E-polarized plane-wave reflectance, transmittance, and absorbance. Still, these resonances, associated to the so-called lattice modes, remain insufficiently investigated.

Therefore, we would like to apply a MAR-RHP solution to the scattering of H-polarized plane wave by a PEC strip grating on a dielectric layer. It can be anticipated that the algorithm obtained will be very efficient and enable us to focus numerical analysis on the lattice-mode resonances. Besides, unlike Nystrom-type discretizations, it should be amenable to analytical solution in the form of asymptotic power series, see [2,9,15,17], suitable for analysis of eigenvalues and associated resonances. Such analysis is envisaged as the next step in our on-going research into the lattice modes.

## 2. Formulation of problem

Consider an infinite flat grating of PEC strips with zero thickness and width  $d$ , located in the plane  $y = 0$  with period  $r$  (Figure 1). This plane is the top interface of a homogeneous dielectric layer (substrate) of the thickness  $h$  and relative dielectric permittivity  $\epsilon$ . The H-polarized plane wave is incident at the angle  $\beta$  and depends on time as  $e^{-i\omega t}$ .

In the case of the  $H$ -polarization, the field components are  $(E_x, E_y, 0)$  and  $(0, 0, H_z)$ . It is convenient to choose  $H_z$  as the "basic" component; we denote it  $U(x, y)$ .

The given incident field is a plane wave,

$$U^{in}(x, y) = e^{-ik_0 y \sin \beta - ik_0 x \cos \beta}, y > 0, \quad (1)$$

where  $k_0 = \omega/c = \omega(\epsilon_0 \mu_0)^{1/2}$ ,  $c = 1/(\epsilon_0 \mu_0)^{1/2}$ . Then the total field is a sum,  $U^{tot} = U^{in} + U^{(1)}$ , in the domain #1, and  $U^{tot} = U^{(2,3)}$  in the domains ##2,3. Thus, we obtain the following boundary value problem for  $U$ :

- (I) it must satisfy the 2-D Helmholtz equation everywhere outside the strips and the slab interfaces,

$$\begin{aligned} (\nabla^2 + k_0^2)U^{(1,3)}(\vec{r}) &= 0, y > 0, y < -h \\ (\nabla^2 + k_0^2 \epsilon)U^{(2)}(\vec{r}) &= 0, -h < y < 0 \end{aligned} \quad (2)$$

- (II) the transmission conditions at the whole lower interface,  $y = -h, x \in \text{Re} : \{-\infty < x < +\infty\}$ ,

$$U^{(2)} = U^{(3)}, \partial U^{(2)}/\epsilon \partial y = \partial U^{(3)}/\partial y, \quad (3)$$

and at the slots  $\vec{r} \in S = \text{Re} \setminus M$  of the upper interface,

$$U^{(1)} + U^{in} = U^{(2)}, (\partial U^{(1)} + \partial U^{in})/\partial y = \partial U^{(2)}/\epsilon \partial y, \quad (4)$$

plus the PEC boundary condition on the strips, i.e.  $\vec{E}_{tg}(\vec{r}) = 0$  at  $\vec{r} \in M : \{y = 0, |x + np| < d, n = 0, \pm 1, \pm 2, \dots\}$ , that means

$$\partial U^{(1)}/\partial y = -\partial U^{in}/\partial y, \quad \partial U^{(2)}/\partial y = 0, \quad (5)$$

- (III) the radiation condition, which means that at  $y \rightarrow \pm\infty$  the scattered field must contain only "outgoing" waves, and  
 (IV) the condition of local finiteness of power: the power, stored in any finite space domain  $D$  tends to zero if  $D \rightarrow 0$ ; this condition determines the edge behavior of the function  $U$ : it must tend to zero as a square root of the distance to the edge.

Additionally, the periodicity of the domain  $M$ , together with the shape of (1), entails the quasi-periodicity property,

$$U(x + p) = e^{-ik_0 p \cos \beta} U(x) \quad (6)$$

Conditions (I)–(IV) provide the uniqueness of the solution: if the function  $U$  exists, then it is unique.

### 3. Dual series equation

Thanks to the quasi-periodicity (6), the scattered field in the upper half-space (domain #1) is sought as a Floquet series,

$$U^{(1)} = \sum_{n=-\infty}^{\infty} a_n e^{i(\gamma_n y + \beta_n x)}, y > 0, \quad (7)$$

the field in the dielectric slab (domain #2) as

$$U^{(2)} = \sum_{n=-\infty}^{\infty} (b_n e^{i\gamma_n^s y} + c_n e^{-i\gamma_n^s y}) e^{i\beta_n x}, 0 > y > -h, \quad (8)$$

and the field in the lower half-space (domain #3) as

$$U^{(3)} = \sum_{n=-\infty}^{\infty} d_n e^{i(-\gamma_n y + \beta_n x)}, y < -h, \quad (9)$$

Here, we have introduced the following notations:

$$\gamma_n = (k_0^2 - \beta_n^2)^{1/2}, \gamma_n^s = (k_0^2 \varepsilon - \beta_n^2)^{1/2}, \beta_n = 2\pi n/p - \beta_0, \quad (10)$$

so that  $\gamma_0 = k_0 \sin \beta$ ,  $\beta_0 = k_0 \cos \beta$ .

The reflectance and transmittance are the power fractions reflected from and transmitted through the slab with grating. They are expressed via the Floquet harmonic amplitudes as

$$P_{ref} = \gamma_0^{-1} \sum_{|n-\kappa \cos \beta| < \kappa} \gamma_n |a_n|^2, P_{tr} = \gamma_0^{-1} \sum_{|n-\kappa \cos \beta| < \kappa} \gamma_n |d_n|^2. \quad (11)$$

where we have denoted  $\kappa = p/\lambda$ . Substituting (7)–(9) into the conditions (3), we obtain

$$\sum_{n=-\infty}^{\infty} (b_n e^{-i\gamma_n^s h} + c_n e^{i\gamma_n^s h}) e^{i\beta_n x} = \sum_{n=-\infty}^{\infty} d_n e^{i\gamma_n h} e^{i\beta_n x}, \quad (12)$$

$$\frac{1}{\varepsilon} \sum_{n=-\infty}^{\infty} (i\gamma_n^s b_n e^{-i\gamma_n^s h} - i\gamma_n^s c_n e^{i\gamma_n^s h}) e^{i\beta_n x} = \sum_{n=-\infty}^{\infty} -i\gamma_n d_n e^{i\gamma_n h} e^{i\beta_n x} \quad (13)$$

Since these series coincide on the entire period, we replace them with term-wise equations and exclude the unknowns  $b_n$  and  $c_n$ , expressing them via  $d_n$ ,

$$b_n = \frac{1}{2} d_n e^{i\gamma_n h} \left( 1 - \frac{\gamma_n \varepsilon}{\gamma_n^s} \right) e^{i\gamma_n^s h}, c_n = \frac{1}{2} d_n e^{i\gamma_n h} \left( 1 + \frac{\gamma_n \varepsilon}{\gamma_n^s} \right) e^{-i\gamma_n^s h} \quad (14)$$

According to the PEC conditions (5) on the strips,  $\vec{r} \in M$ ,

$$\sum_{n=-\infty}^{\infty} (i\gamma_n^{sl} b_n - i\gamma_n^{sl} c_n) e^{i\beta_n x} = 0, \quad (15)$$

$$-k_0 \sin \beta e^{i\beta_0 x} + \sum_{n=-\infty}^{\infty} \gamma_n a_n e^{i\beta_n x} = 0. \quad (16)$$

On the slots,  $\vec{r} \in S$ , the conditions (4) yield

$$e^{i\beta_0 x} + \sum_{n=-\infty}^{\infty} a_n e^{i\beta_n x} = \sum_{n=-\infty}^{\infty} (b_n + c_n) e^{i\beta_n x} \quad (17)$$

$$-k_0 \sin \beta e^{i\beta_0 x} + \sum_{n=-\infty}^{\infty} a_n \gamma_n e^{i\beta_n x} = \frac{1}{\varepsilon} \sum_{n=-\infty}^{\infty} (\gamma_n^{sl} b_n - \gamma_n^{sl} c_n) e^{i\beta_n x} \quad (18)$$

Thanks to (15) and (16), Equation (18) is satisfied on the entire period. Therefore, on substituting  $b_n$  and  $c_n$  from (14) and introducing new coefficients ( $n = 0, \pm 1, \dots$ ),

$$M_n = -\delta_{n,0} k_0 \sin \beta + \gamma_n a_n, \quad (19)$$

where  $\delta_{n,0}$  is the Kroenecker symbol, we see that

$$d_n = M_n \varepsilon e^{i\gamma_n h} [i\gamma_n^{sl} \sin(\gamma_n^{sl} h) + \gamma_n \varepsilon \cos(\gamma_n^{sl} h)]^{-1} \quad (20)$$

On denoting  $\phi = 2\pi x/p$  and  $\theta = \pi d/p$  and introducing

$$\Gamma_n = \frac{p}{2\pi} \left[ \frac{1}{\gamma_n} - \frac{\varepsilon}{\gamma_n^{sl}} \frac{(\gamma_n^{sl} - \gamma_n \varepsilon) e^{i\gamma_n^{sl} h} + (\gamma_n^{sl} + \gamma_n \varepsilon) e^{-i\gamma_n^{sl} h}}{(\gamma_n^{sl} - \gamma_n \varepsilon) e^{i\gamma_n^{sl} h} - (\gamma_n^{sl} + \gamma_n \varepsilon) e^{-i\gamma_n^{sl} h}} \right]^{-1}, \quad (21)$$

the expression (17) enables us to derive a dual series equation,

$$\begin{cases} \sum_{n=-\infty}^{\infty} x_n \Gamma_n e^{in\phi} = 2\Gamma_0, & \theta < |\phi| \leq \pi, \\ \sum_{n=-\infty}^{\infty} x_n e^{in\phi} = 0, & |\phi| < \theta, \end{cases} \quad (22)$$

where new unknowns are

$$x_0 = M_0(\Gamma_0)^{-1} + 2, \quad x_n = M_n(\Gamma_n)^{-1}. \quad (23)$$

Note that, if  $|n| \rightarrow \infty$ , then the weight function in (22) behaves as  $\Gamma_n = i(1 + \varepsilon)^{-1}|n| [1 + O(1/|n|) + O(e^{-|n|2\pi h/p})]$ .

#### 4. Regularization of DSE

To make analytical regularization, we introduce

$$\Delta_n = |n| + i(1 + \varepsilon)\Gamma_n \quad (24)$$

and cast DSE (22) to the canonical form,

$$\left\{ \begin{array}{l} \sum_{n=-\infty}^{\infty} x_n |n| e^{in\phi} = \sum_{n=-\infty}^{\infty} x_n \Delta_n e^{in\phi} - i(1 + \varepsilon)2_0, \theta < |\phi| \leq \pi, \\ \sum_{n=-\infty}^{\infty} x_n e^{in\phi} = 0, \quad |\phi| < \theta, \end{array} \right. \quad (25)$$

The left-hand part of (25) forms the RHP on the unit circle, solution of which is known and expressed via the Plemelj-Sokhotskii formulas. Details of this procedure can be found, for instance, in [28,8,9,15]; note that it exploits explicitly the edge condition (IV). When applied to the full Equation (22), this yields an infinite matrix equation,

$$x_m = \sum_{n=-\infty}^{\infty} A_{mn} x_n + B_m, \quad m = 0, \pm 1, \pm 2, \dots \quad (26)$$

$$A_{mn} = \Delta_n(\kappa, \varepsilon, h/p) T_{mn}(\theta), \quad B_m = -i(1 + \varepsilon)2_0 T_{m0}(\theta), \quad (27)$$

The functions  $T_{mn}(\theta)$  are expressed via the Legendre polynomials  $P_m$  of the argument  $u = -\cos \theta$ , see [28,8,9],

$$T_{mn}(\theta) = \frac{(-1)^{m+n}}{2(m-n)} [P_m(u)P_{n-1}(u) - P_{m-1}(u)P_n(u)], \quad m \neq n, \quad (28)$$

$$T_{00}(\theta) = -\ln \frac{1}{2}(1 + \cos \theta), \quad (29)$$

$$T_{mm}(\theta) = \frac{1}{2|m|} \left[ 1 + \sum_{s=1}^{|m|} t_s(u) P_{s-1}(u) \right], \quad m \neq 0, \quad (30)$$

where  $t_0 = 1$ ,  $t_1(u) = -u$ ,  $t_s(u) = P_s(u) - 2uP_{s-1}(u) + P_{s-2}(u)$ .

The large-index asymptotics of the Legendre polynomials allow seeing that the following inequalities hold true:

$$\sum_{m,n=-\infty}^{+\infty} |A_{mn}|^2 < \infty, \quad \sum_{m=-\infty}^{+\infty} |B_m|^2 < \infty, \quad (31)$$

Hence, Equation (26) is a Fredholm second-kind matrix equation in the space of number sequences  $l_2$  and hence the convergence of its numerical solution for progressively larger truncation numbers is mathematically guaranteed. Note that expressions (27) are combinations of elementary functions, need no numerical integrations, and hence can be easily computed with machine precision. This is an advantage before the other MAR-like techniques, such as [3–5,14,20–27].

Inspection of (24) and (27) shows that both  $\Delta_n$  and  $A_{mn}$  are proportional to the normalized frequency,  $\kappa = p/\lambda$ . This means that the regularization, i.e. semi-inversion of DSE, is performed via the analytical inversion of the static part.

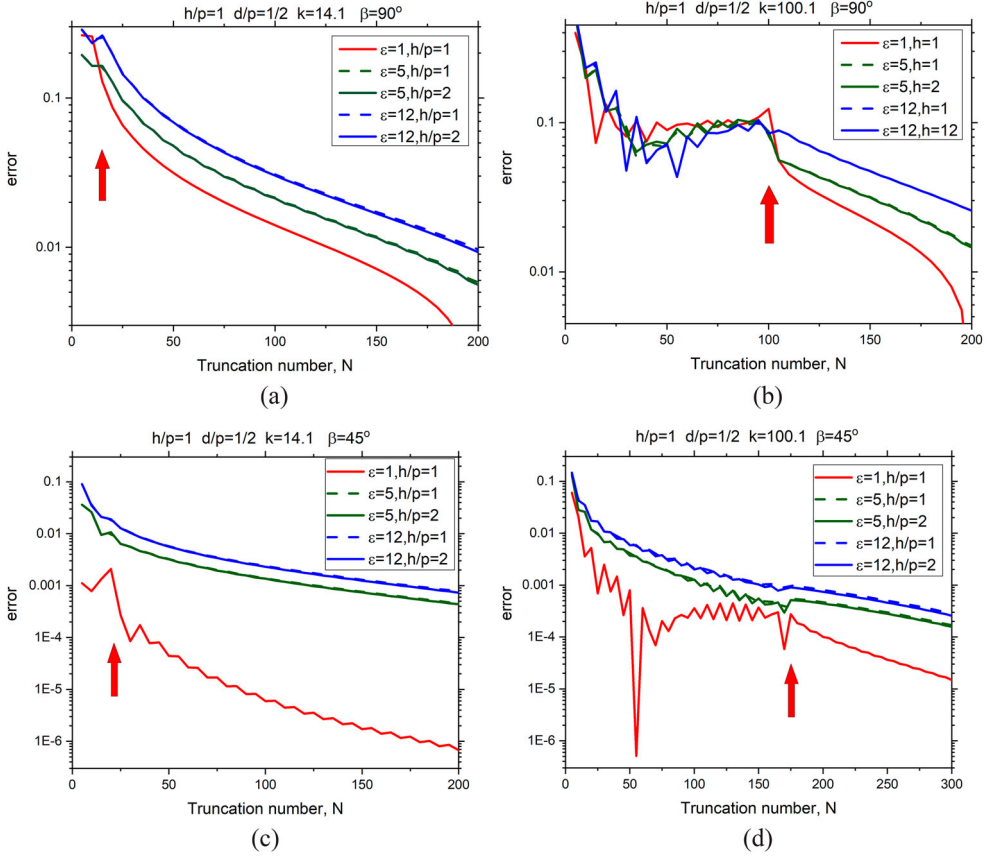


**Figure 2.** The error, in the  $l_2$ -norm, in the computation of unknown coefficients versus the matrix truncation order for the grating with  $\beta = 90^\circ$  and  $45^\circ$ ,  $d/p = 0.5$ , and different parameters  $\varepsilon$  and  $h/p$ , as indicated in the inset. The normalized frequency is  $\kappa = 14.1$  for (a) and (c), and  $\kappa = 100.1$  for (b) and (d).

## 5. Convergence and validation

To visualize the convergence of the numerical solution, we consider normal and inclined incidence,  $\beta = 90^\circ$  and  $45^\circ$ , and select two values of the normalized frequency  $\kappa = p/\lambda$ , namely 14.1 and 100.1. We compute the relative error, in the  $l_2$ -norm, of the solution found with varying truncation order  $N$  as compared to  $N = 400$ , for several values of the grating and slab parameters,

$$e_x(N) = \left( \sum_{n=-400}^{400} |x_n^N - x_n^{400}|^2 \right)^{1/2} \left( \sum_{n=-400}^{400} |x_n^{400}|^2 \right)^{-1/2} \quad (32)$$

This value can be considered as the near-field error. As one can see from Figure 2, it starts exponential decay as soon as  $N$  becomes larger than  $\kappa + 5$ .

In the analysis of the wave scattering from gratings, normally the phenomena of reflection and transmission, in terms of the power, are interested in. Therefore, we define and

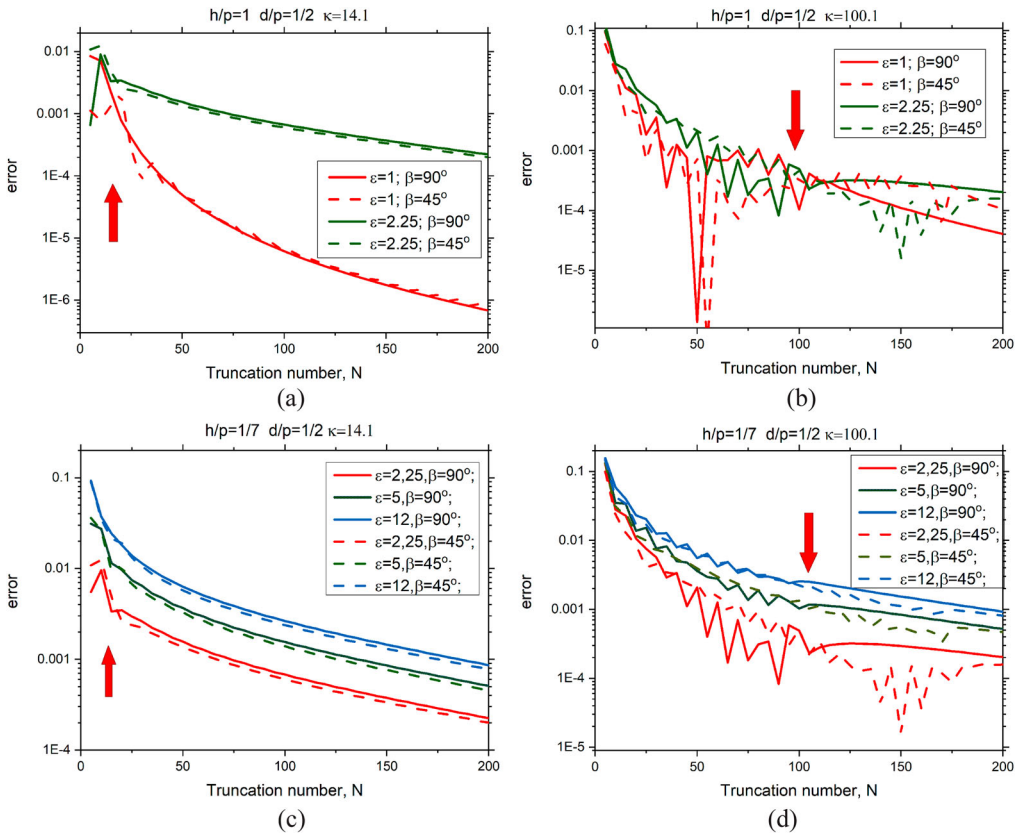


**Figure 3.** The far-field error versus the order of truncation for the grating with  $d/p = 0.5$ , angle of incidence  $\beta = 90^\circ$  and  $45^\circ$ , and  $h/p$  and  $\epsilon$  as indicated.  $\kappa = 14.1$  (a), (c) and  $\kappa = 100.1$  (b), (d).

compute the far-field error as a function of  $N$ ,

$$e_\sigma(N) = |\sigma_N - \sigma_{400}| / \sigma_{400}, \quad (33)$$

where  $\sigma$  is either transmittance or reflectance, given in (11).

The results of computations are shown in Figure 3. With an increase in the truncation order  $N$  over  $\kappa$ , which is marked by red arrows, the error decreases, i.e. the accuracy of the calculation increases. As visible, the rate of convergence is the highest in the case of absence of dielectric layer, while thicker and optically denser slabs entail larger values of  $N$  to achieve the same accuracy. In contrast, the fill factor,  $d/p$ , and the angle of incidence,  $\beta$ , do not change the rate of convergence.

As a proof of validation, we present, in Figure 4, the comparison of our results with those of [25], computed by a different accurate technique, MAR-Galerkin with Chebyshev's polynomials. Here, we show the absolute value of the reflectance of PEC strip grating on top of dielectric substrate versus the frequency in the range  $\kappa \leq 1$ , where only the 0-th Floquet harmonic of the scattered field is radiating. The data for freestanding strip array and for unloaded dielectric slab are also shown. The corresponding curves visually overlap that is understandable because both methods are convergent and the orders of discretization



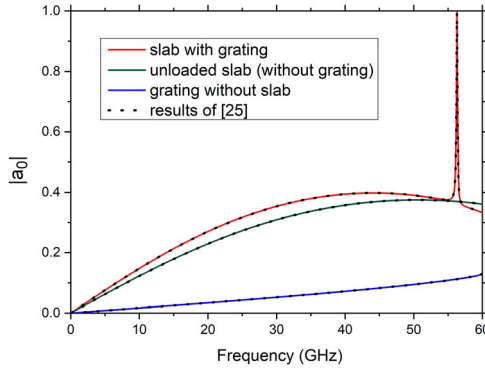


**Figure 4.** Comparison of the results of [25] and MAR-RHP using (26), for  $p = 5$  mm,  $d = 1$  mm,  $h = 1$  mm,  $\varepsilon = 2.2$  (i.e.  $d/p = h/p = 0.2$ ). Absolute value of the amplitude reflection coefficient of strip grating on top of dielectric substrate versus the frequency in the single-mode range,  $0 < \kappa < 1$ . The plots for freestanding strip array and for bare dielectric slab are also shown.

provide 4–5 correct digits. A striking feature of the plot for the narrow-strip ( $d = 0.2p$ ) grating on the thin ( $h = 0.2p$ ) dielectric slab is a sharp total-reflection peak at 57 GHz. This is a resonance on the lattice mode, discussed below. Off resonance, the reflection is almost the same as for a bare slab.

## 6. Numerical results: lattice-mode resonances

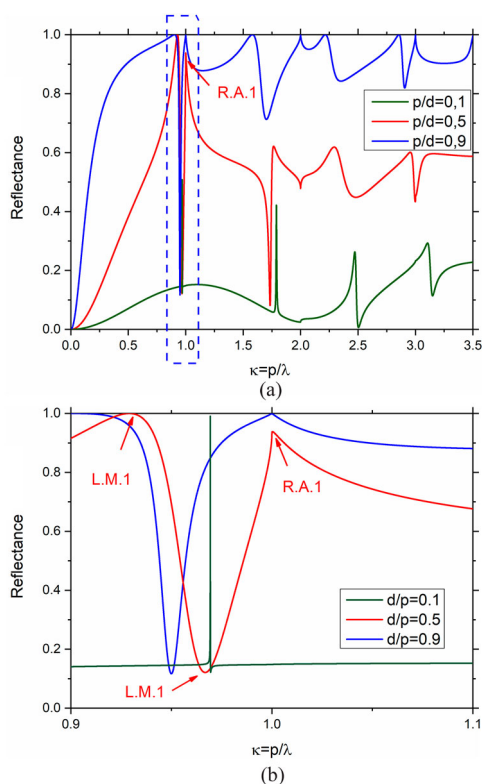
On the verification of our code, we present, in Figure 5(a), the plots of the reflectance (11) as a function of the normalized frequency, for three values of the strip width-to-period ratio,  $d/p = 0.9, 0.5$  and  $0.1$ , for the normal incidence. Note the sharp bends of all curves exactly at  $\kappa = 1, 2, 3$  due to the Rayleigh anomalies (RA) of the  $\pm n$ -th index, which are the roots of equations  $\gamma_n = 0$ ,  $n = \pm 1, \pm 2, \dots$  at  $\cos \beta = 0$ . At lower frequency values, one can see the Fano-shape double extrema due to the resonances on the lattice modes of the  $\pm 1$ -st and higher orders, respectively.

Figure 5(b) is a zoom of the vicinity of the 1-st RA. As visible, if the PEC strips are narrow ( $d < p$ ), then the reflectance is low however in the resonance on the lattice mode it becomes total, in a narrow range. Still, for half-period and wider strips ( $d \geq p/2$ ), the reflection is high everywhere except of the vicinity of the lattice-mode resonance, where it drops to a low value. Thus, a PEC-strip grating on a thin dielectric substrate is able to demonstrate both extraordinary full-reflection and extraordinary full-transmission effects, in the lattice-mode resonances.

These and other results presented below have been computed with truncation number  $N = 50$  that provide 8 or more correct digits in the reflectance at all studied frequencies.

To investigate the resonances on the lattice modes, we plot, in Figure 6, the curves of the reflectance (11) as a function of the normalized frequency  $\kappa$ , for the H-polarized plane wave, normally incident on a grating with equal strips and slots and two values of relative dielectric permittivity, 2.2 (Teflon, Polyethylene) and 3.8 (fused quartz). The plot of the same quantity for a grating without substrate ( $\varepsilon = 1$ ) is also shown for comparison.

Sharp resonances slightly below the RA wavelengths at the normal incidence, are well visible. However, they are absent if the dielectric slab is absent, i.e. PEC strip grating is



**Figure 5.** The reflectance of the on-substrate grating versus the normalized frequency for  $h/p = 1/7$ ,  $\varepsilon = 2.25$  (Teflon, Polyethylene), and three values of the filling factor, i.e. the strip-to-period ratio (a), and the zoom of (a) in the marked interval near  $\kappa = 1$  (b).

suspended in the free space. On the panels (b) and (c), we show the zooms of the vicinities of the 1-st and the 2-nd RA, respectively.

At the frequencies, corresponding to the lattice resonances, we visualize the near field patterns – see Figures 7 and 8. Here, as the resonances have Fano shapes, each pair of patterns corresponds to the frequencies of the maximum (a) and the minimum (b) reflectance. Therefore, on panels (a) one can see the standing wave created by the interference of the incident plane wave and the strongly reflected wave (i.e. the 0-th Floquet harmonic) in the upper half-space and deep shadow in the lower half-space. The slab is depicted using white dashes.

In the domain of slab, the lattice-mode contribution clearly dominates on both panels. In Figure 7, there are two bright spots of the field on a period, while in Figure 8 there are six spots. This indicates that the resonating modes are  $L_1$  and  $L_3$ , respectively.

The standing-wave pattern, characteristic for the lattice modes, is created by the equal-amplitude  $+1$ -st and  $-1$ -st Floquet harmonics, and  $+3$ -rd and  $-3$ -rd, respectively. This happens because the mentioned harmonics are synchronized, in the resonance, with the principal natural (guided) wave of the dielectric slab, in terms of the phase velocity (or the natural-wave wavelength) along the  $x$ -axis.

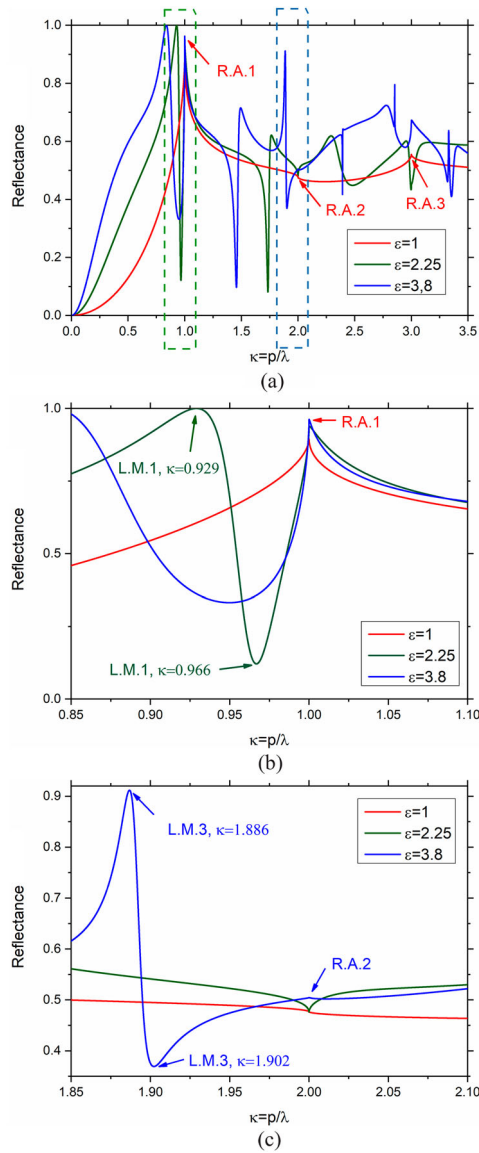


**Figure 6.** The same as in Figure 5 however, for  $d/p = 0.5$ ,  $h/p = 1/7$ , and three values of the permittivity,  $\epsilon = 1, 2.25$ , and  $3.8$  (fused quartz) (a), and the zooms of (a) in the marked intervals near  $\kappa = 1$  (b), and  $\kappa = 2$  (c).

It should be emphasized that the lattice or grating modes are attracting great attention today. This is because they are responsible for a number of amazing and sometimes counter-intuitive phenomena, such as “anomalous” transmission and, reciprocally, reflection, and enhanced absorption in the case of lossy gratings, plus giant Kerr, Kerker, and Faraday effects [29–32]. The existence of the lattice modes is caused by the periodicity. Their optical properties, for the strip and wire gratings in the visible-light wavelength range were recently reviewed in [33]; another review, with emphasis on experimental measurements, can be found in [34].

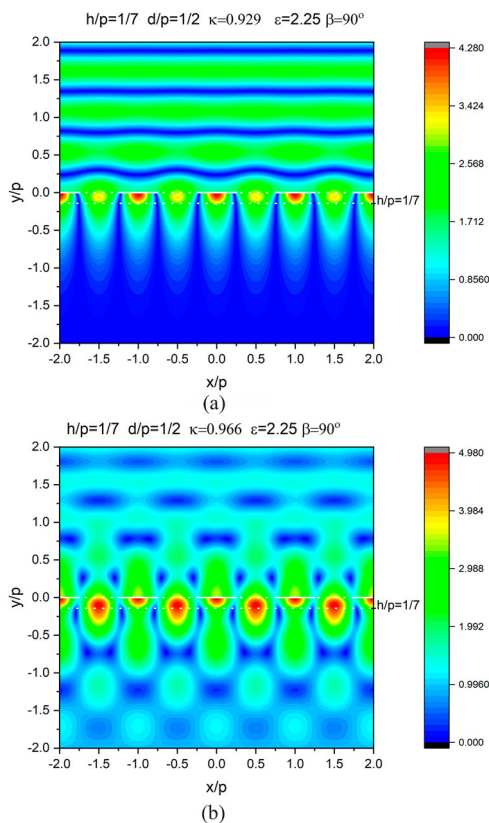


**Figure 7.** Near magnetic field patterns on three periods of the PEC strip grating on top of dielectric slab with  $\varepsilon = 2.25$ , in the maximum  $\kappa = 0.929$  (a) and in the minimum  $\kappa = 0.966$  (b) of reflectance, corresponding to the Fano-shape resonance on the  $L_1$  mode, see Figure 6(b).

What is amazing, sharp lattice-mode resonances were first observed experimentally over 50 years ago when the “phased-array blindness effect” was discovered [35,36].

As already mentioned, the lattice modes, i.e. the poles of the field  $U$  as a function of the normalized frequency,  $\kappa$ , and associated with them resonances are absent in the case of zero-thickness PEC-strip grating in the free space, i.e. without finite-thickness dielectric substrate. This is apparently the reason that the corresponding effects are sometimes called “guided-mode resonances.” Still, as soon as the strips are assumed not PEC, the resonances on the lattice modes emerge near to the Rayleigh anomalies as the dominant features in the scattering and absorption [9,15,16,24,26,33]. The same happens if the strips have however small but finite thickness.

Here, the existence of the natural guided waves of dielectric substrate or non-PEC plane (such as graphene plane) plays the role of mediator. They shift the lattice-mode poles further to the red from the RA values according to the wavelength of the natural wave, which is always shorter than the free-space wavelength.

Finally, we present the results related to the inclined incidence of the plane H-polarized wave on the PEC strip grating on top of a dielectric substrate layer, see Figure 9.

In this case, each Rayleigh anomaly splits to two anomalies  $+m$ -th and  $-m$ -th, according to two separate roots of equations  $\gamma_n = 0$ ,  $n = \pm 1, \pm 2, \dots$  at  $\cos \beta \neq 0$ . One of the RA, for

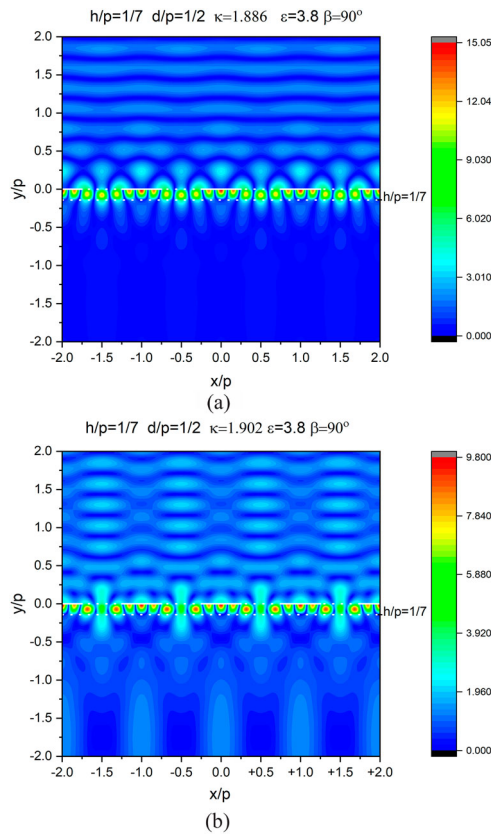


**Figure 8.** The same as Figure 7, however, for  $\varepsilon = 3.8$  and the resonance on the  $L_3$  mode in the maximum  $\kappa = 1.886$  (a) and in the minimum  $\kappa = 1.902$  (b) of the reflectance, see Figure 6(c).

positive  $n$ , obtains higher, in frequency, value, than at the normal incidence, and the other RA, for negative  $n$ , obtains lower value. Each of the split RA is accompanied with its own “satellite” in the form of the lattice-mode resonance of the same index. They have opposite symmetry with respect to the center of the strip and therefore only one of them, on the symmetric mode, is present at the normal incidence, while the other one, on the anti-symmetric sister mode, is absent. In other words, the anti-symmetric lattice mode remains “dark” at the normal incidence, while symmetric one is “bright.” At inclined incidence, both lattice modes are bright.

These effects are especially well observable if the stripwidth-to-period ratio is close to 1 (see panel (a)) or to zero (see panel (b)). The resonances reveal themselves as sharp and deep drops in reflection and even sharper peaks of reflection, respectively. This corresponds to what is frequently called “anomalous transmission” and “anomalous reflection” phenomena, respectively.

## Conclusions

We have considered the H-polarized plane wave scattering by the infinite grating of zero-thickness PEC strips on the top of dielectric substrate. Our full-wave treatment is based on

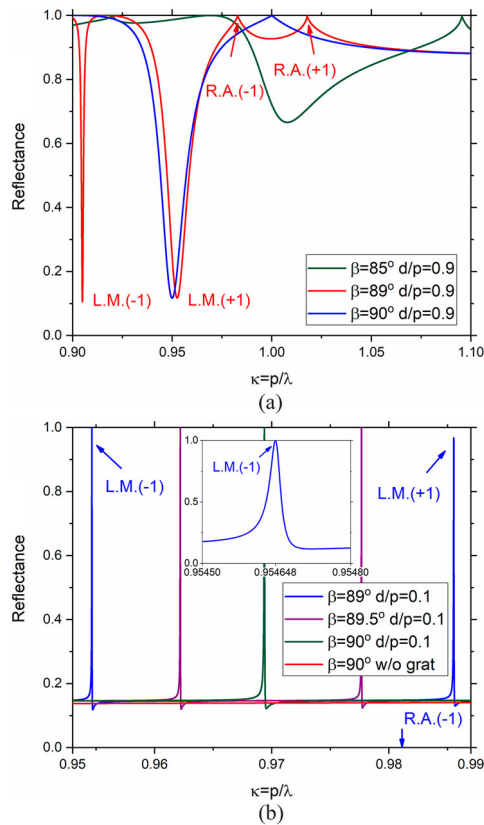


**Figure 9.** The reflectance of the on-substrate grating versus the normalized frequency for  $h/p = 1/7$  and  $\varepsilon = 2.25$  in the case of the normal and inclined incidence, the values of the incidence angle  $\beta$  and the filling factor  $d/p$  are indicated in the insets.

the analytical inversion of the problem static part with the aid of RHP technique. Convergence of the resulting meshless numerical algorithm has been demonstrated and validation of the computed results has been performed by the comparison with data obtained using another convergent technique, MAR-Galerkin. The computations have revealed high-Q resonances on the lattice modes, which do not exist on the PEC-strip grating placed in the free space. These resonances can take form of total reflection and total transmission, depending on the strip width-to-period ratio.

## Disclosure statement

No potential conflict of interest was reported by the author(s).

## Notes on contributors

**Fedir O. Yevtushenko** was born in 1995 in Kharkiv, Ukraine. He received the B.S. and M.S. degrees in photonics and optoinformatics from the National University of Radio Electronics, Kharkiv, Ukraine, in 2017 and 2019, respectively. Currently he is Ph.D. student and part-time Junior Scientist at the Laboratory of Micro and Nano Optics (LMNO), Institute of Radio-Physics and Electronics of the National

Academy of Sciences of Ukraine (IRE NASU), Kharkiv. His research interests are in the wave scattering from gratings, made of perfect and imperfect flat strips and the method of analytical regularization. He was recipient of Young Scientist Prize of the European Microwave Association at the IEEE Ukraine Conference on Electrical and Computer Engineering (UKRCON-2019), Lviv, 2019 and Young Scientist Special Grant of the International Conference on Microwaves, Communications, Antennas, and Electronic Systems (COMCAS-2019), Tel Aviv, 2019.

**Sergii V. Dukhopelnykov** was born in Kharkiv, Ukraine in 1982. He received the B.S., M.S. and Ph.D. degrees in mathematical modeling and numerical methods from the V. N. Karazin Kharkiv National University in 2003, 2004 and 2010, respectively. From 2007 to 2018, he was a Lecturer, Senior Lecturer and Assistant Professor at the Department of Mathematics, National Technical University "Kharkiv Polytechnic Institute" in Kharkiv, Ukraine. Since 2018, he is Senior Scientist at LMNO, IRE NASU, Kharkiv and part-time Assistant Professor at the School of Mathematics of the V. N. Karazin Kharkiv National University. His research interests are in singular integral equations, Nystrom methods, and patterned graphene scattering. He was recipient of the Ph.D. scholarship award of the N. I. Akhizezer Foundation, Kharkiv (2010) and the Young Scientist Prize of the International Conference on Mathematical Methods in Electromagnetic Theory (2018).

**Alexander I. Nosich** was born in 1953 in Kharkiv, Ukraine. He received the M.S., Ph.D., and D.Sc. degrees in radio physics from the V. N. Karazin Kharkiv National University, Ukraine, in 1975, 1979, and 1990, respectively. Since 1979, he has been with IRE NASU, Kharkiv, where he is currently Professor, Principal Scientist and Head, Laboratory of Micro and Nano Optics. Since 1992, he held many guest fellowships and professorships in the EU, the UK, Japan, Singapore, and Turkey. His research interests include the method of analytical regularization, propagation and scattering of waves, open waveguides, antennas and lasers, and the history of microwaves. Prof. Nosich was initiator and technical committee chairman of the international conference series on Mathematical Methods in Electromagnetic Theory (MMET), held in Ukraine since 1990. In 1995, he organized the IEEE AP-S East Ukraine Chapter, the first one in the former USSR. Currently he represents Ukraine in the European Association on Antennas and Propagation. He was awarded the honorary title of Doctor Honoris Causa of the University of Rennes 1, France in 2015 and the Galileo Galilei Medal of the International Commission for Optics in 2017, and elected Fellow of IEEE in 2003 and Fellow of the Optical Society (OSA) in 2019. He was also co-recipient the 2017 National Prize of Ukraine in Science and Technology for the works entitled, "Photonics of semiconductor and dielectric nanostructures" and the 2018 Solomon I. Pekar Award of NASU in the solid state physics theory.

## References

- [1] Lamb H. On the reflection and transmission of electric waves by a metallic grating. *Proc London Math Soc.* **1898**;29:523–544.
- [2] Nosich AI. Method of analytical regularization in computational photonics. *Radio Sci.* **2016**;51(8):1421–1430.
- [3] Yampolsky VG. Diffraction of a plane electromagnetic wave by an array of metallic strips. *Radio Eng Electron Phys.* **1963**;8(4):564–572.
- [4] Matsushima A, Itakura T. Singular integral equation approach to plane wave diffraction by an infinite strip grating at oblique incidence. *J Electromagn Waves Appl.* **1990**;4(6):505–551.
- [5] Matsushima A, Zinenko TL, Nishimori H, et al. Plane wave scattering from perpendicularly crossed multilayered strip gratings. *Progress Electromagn Res.* **2000**;28:185–203.
- [6] Lucido M. An analytical technique to fast evaluate mutual coupling integrals in spectral domain analysis of multilayered coplanar coupled striplines. *Microw Opt Technol Lett.* **2012**;54(4):1035–1039.
- [7] Lucido M. An efficient evaluation of the self-contribution integrals in the spectral-domain analysis of multilayered striplines. *IEEE Antennas Wirel Propag Lett.* **2013**;12:360–363.
- [8] Agranovich ZS, Marchenko VA, Shestopalov VP. Diffraction of a plane electromagnetic wave from plane metallic lattices. *Sov Phys Techn Phys.* **1962**;7(1):277–286.

- [9] Zinenko TL, Nosich AI, Okuno Y. Plane wave scattering and absorption by resistive-strip and dielectric-strip periodic gratings. *IEEE Trans Antennas Propag.* **1998**;46(10):1498–1505.
- [10] Tsalamengas JL, Fikioris JG, Babili BT. Direct and efficient solutions of integral equations for scattering from strips and slots. *J Appl Phys.* **1989**;66(1):69–80.
- [11] Kaliberda ME, Lytvynenko LM, Pogarsky SA. Singular integral equations in diffraction problem by an infinite periodic strip grating with one strip removed. *J Electromagn Wave Appl.* **2016**;30(18):2411–2426.
- [12] Gandel YV, Polyanskaya TS. Justification of a numerical method for solving systems of singular integral equations in diffraction grating problems. *Differ Equations.* **2003**;39(9):1295–1307.
- [13] Tsalamengas JL. Quadrature rules for weakly singular, strongly singular, and hypersingular integrals in boundary integral equation methods. *J Comput Phys.* **2015**;303:498–513.
- [14] Matsushima A, Zinenko TL, Minami H, et al. Integral equation analysis of plane wave scattering from multilayered resistive strip gratings. *J Electromagn Waves Appl.* **1998**;12(11):1449–1469.
- [15] Zinenko TL, Nosich AI. Plane wave scattering and absorption by flat gratings of impedance strips. *IEEE Trans Antennas Propag.* **2006**;54(7):2088–2095.
- [16] Zinenko TL, Marciniak M, Nosich AI. Accurate analysis of light scattering and absorption by an infinite flat grating of thin silver nanostrips in free space using the method of analytical regularization. *IEEE J Sel Top Quantum Electron.* **2013**;19(3):art. no 9000108.
- [17] Tretyakov OA, Shestopalov VP. Electromagnetic wave diffraction by a plane metal grating lying on a dielectric layer. *Izv VUZov Radiofizika.* **1963**;5(2):353–363.
- [18] Panin SB, Poyedinchuk AY. Electromagnetic wave diffraction by a grating with a chiral layer. *Radiophys Quantum Electron.* **2002**;45(8):629–639.
- [19] Panin SB, Vinogradova ED, Poyedinchuk AY, et al. Resonant diffraction from a grating on a paramagnetic layer with frequency dispersion. *Progress Electromagn Res M.* **2009**;6:185–199.
- [20] Matsushima A, Fujimura T, Itakura T. Scattering of an arbitrary plane wave by an infinite strip grating loaded with a pair of dielectric slabs. *J Electromagn Waves Appl.* **1993**;7(6):791–809.
- [21] Matsushima A, Itakura T. Polarization diplexing by a double strip grating loaded with a pair of dielectric slabs. *IEICE Trans Electron.* **1993**;E76-C(6):486–495.
- [22] Volakis JL, Lin YC, Anastassiou H. TE characterization of resistive strip gratings on a dielectric slab using single-mode expansion. *IEEE Trans Antennas Propag.* **1994**;42(2):205–212.
- [23] Cho YK, Cho UH. TM-polarized electromagnetic scattering from a periodic strip array on a grounded dielectric. *Microw Opt Technol Lett.* **1996**;11(1):41–45.
- [24] Zinenko TL, Matsushima A, Okuno Y. Scattering and absorption of electromagnetic plane waves by a multilayered resistive strip grating embedded in a dielectric slab. *Trans IEICE Electron.* **1999**;E82-C(12):2255–2264.
- [25] Rodriguez-Berral R, Medina F, Mesa F, et al. Quasi-analytical modeling of transmission/reflection in strip/slit gratings loaded with dielectric slabs. *IEEE Trans Microw Theory Tech.* **2012**;60(3):405–418.
- [26] Zinenko TL, Matsushima A, Nosich AI. Surface-plasmon, grating-mode and slab-mode resonances in THz wave scattering by a graphene strip grating embedded into a dielectric slab. *IEEE J Sel Top Quantum Electron.* **2017**;23(4):art. no 4601809.
- [27] Medina F, Mesa F, Skigin DC. Extraordinary transmission through arrays of slits: a circuit theory model. *IEEE Trans Microw Theory Tech.* **2010**;58(1):105–115.
- [28] Nosich AI. Green's function – dual series approach in wave scattering from combined resonant scatterers. In: Hashimoto M, MM Idemen, OA Tretyakov, editors. *Analytical and numerical methods in electromagnetic wave theory.* Tokyo: Science House Publ; **1993.** p. 419–469.
- [29] Wang J, Li H, Cao X, et al. Properties of grating modes and their effect on reflection behavior of a periodic array of parallel rods by modal method. *J Appl Phys.* **2015**;118(10):art. no 103109.
- [30] Belotelov VI, Akimov IA, Pohl M, et al. Enhanced magneto-optical effects in magnetoplasmonic crystals. *Nat Nanotechnol.* **2011**;6:370–376.
- [31] Babicheva VE, Evlyukhin AB. Resonant lattice Kerker effect in metasurfaces with electric and magnetic optical responses. *Laser Photon Rev.* **2017**;11(6):art. no 1700132.



- [32] Yachin VV, Zinenko TL, Mizrakhy SV. Resonance enhancement of Faraday rotation in double-periodic gyromagnetic layers analyzed by the method of integral functional. *J Opt Soc Am B*. [2018](#);35(4):851–860.
- [33] Zinenko TL, Byelobrov VO, Marciniak M, et al. Grating resonances on periodic arrays of sub-wavelength wires and strips: from discoveries to photonic device applications. In: O Shulika, I Sukhoivanov, editor. *Contemporary optoelectronics: materials, metamaterials and device applications*. Berlin: Springer Ser. Opt. Sci.; [2016](#). vol. 199, p. 65–79.
- [34] Kravets VG, Kabashin AV, Barnes WL, et al. Plasmonic surface lattice resonances: a review of properties and applications. *Chem Rev*. [2018](#);118:5912–5951.
- [35] Oliner AA. On blindness in large phased arrays. *Alta Frequenza*. [1969](#);38(Special Issue):221–228.
- [36] Pozar DM, Schaubert DH. Scan blindness in infinite phased arrays of printed dipoles. *IEEE Trans Antennas Propag*. [1984](#);32(6):602–610.